Transit time of optical pulses propagating through a finite length medium

Mark Bloemer,[1,*] Krishna Myneni,[2] Marco Centini,[1,3] Michael Scalora,[1] and Giuseppe D'Aguanno[1,3]
[1]*U.S. Army Aviation and Missile Command, Research, Development, and Engineering Center, AMSAM-RD-WS-ID, Redstone Arsenal, Alabama 35898*
[2]*Science Applications International Corporation, 6725 Odyssey Drive, Huntsville, Alabama 35806*
[3]*INFM, Dipartimento di Energetica, La Sapienza, University of Rome, Via A. Scarpa 14, 00161 Rome, Italy*
(Received 5 November 2001; revised manuscript received 14 February 2002; published 20 May 2002)

We present experimental and theoretical results on the transit time of optical pulses propagating through bulk media of finite length, specifically GaAs and silica. The transit time of the peak of the pulse varies with the central wavelength due to the étalon effects caused by the reflectivity at the air/medium boundaries. For transform limited optical pulses, the transit time as a function of wavelength follows the transmittance spectrum, that is, the longest transit time occurs at the transmittance maxima where the cavity dwell time is the longest and the shortest transit time occurs at the transmittance minima. The results are dramatically different for chirped pulses obtained by modulating the injection current of a diode laser. The range in the transit times for chirped pulses is a factor of four times larger compared with transform limited pulses. In addition, the transit time for chirped pulses propagating through the GaAs sample is negative at certain wavelengths. Also, the transmitted pulse is not distorted. Although modulating the injection current of a diode laser is the most common method for generating optical pulses, to our knowledge this is the first reported observation of the transit time of these chirped optical pulses propagating through a simple étalon structure.

DOI: 10.1103/PhysRevE.65.056615 PACS number(s): 42.25.Bs, 42.50.Md, 42.25.Hz

I. INTRODUCTION

Propagation of electromagnetic pulses in a dispersive medium has been a topic of scientific and practical interest for over 100 years. The first controversy in the field took place shortly after the development of the theory of special relativity. It was known that the group velocity of an electromagnetic pulse (the velocity of the peak of the pulse) could be greater than c, the speed of light in vacuum, for the case of anomalous dispersion. Within a short time, Sommerfeld was able to show that a group velocity greater than c did not violate special relativity. The reason was that a group velocity greater than c was associated with a transmittance of less than unity. Therefore, the identification of the group velocity with the energy velocity breaks down, and in all cases the velocity at which a signal propagates will never exceed c. This implies that the leading edge of the transmitted pulse is never ahead of the leading edge of a pulse that propagated through vacuum. This early work on propagation in a dispersive medium is still highly relevant today and is summarized in Brillouin's book [1].

In a later work by Garrett and McCumber [2] on the propagation of a Gaussian light pulse through an absorptive medium, it was shown that the classical expression for the group velocity gives the correct result even in the case of group velocities greater than c or negative group velocities. Also worthy of note was their result that if the spectral width of the input Gaussian pulse is much smaller than that of the absorption line, then the pulse remains substantially Gaussian and unchanged in width for many exponential absorption depths.

Before proceeding further, we define a word that is in common usage today: *superluminal*. We prefer the definition of superluminal used in Ref. [3], a pulse propagation velocity that exceeds the group velocity in the (linear) bulk medium. It is often implied that the group velocity is superluminal only if the group velocity exceeds c. While the value of c is an absolute reference point, nevertheless it is arbitrary. More importantly, a reference of the group velocity in relation to the speed of light in vacuum gives the misleading impression that something unusual is happening if the group velocity exceeds c.

In addition to anomalous dispersion, a pulse propagating through a saturable gain medium can also be superluminal. In the case of saturable gain, the leading edge of the pulse can be amplified above the original peak height giving superluminal behavior [3]. Therefore, as the pulse shape evolves, the peak of the pulse propagates at superluminal velocities. Even in the case of a gain medium, the group velocity remains a very useful quantity because it correctly predicts the speed at which the peak of the electromagnetic pulse propagates. This also holds for the case of single photon tunneling [4]. As long as all pertinent parameters are identified in conjunction with the group velocity, such as transmittance, reshaping of the original pulse, and its spectral content, the group velocity description continues to be a valid tool.

A more recent result shows that the group velocity is equal to the energy velocity only if the transmittance is unity [5]. For a transmittance of less than unity, the group velocity is equal to the ratio of the energy velocity to the transmittance, $V_g = V_E/T$. If we neglect the case of a gain medium, then V_E never exceeds c, and group velocities greater than c are only possible if energy is lost during the transit of the pulse.

Practical interest in the subject of electromagnetic pulse propagation in a dispersive medium began with radio and radar, and continues today for satellite communications and

*Electronic address: Mark.Bloemer@ws.redstone.army.mil

fiber optic networks. With the advent of microfabrication and nanofabrication techniques, areas such as photonic band gap (PBG) engineering [6] have created a need to examine electromagnetic pulse propagation in materials with strong *geometrical dispersion*. For an electromagnetic wave propagating through a uniform bulk medium, the refractive index and physical distance traversed determine the phase accumulated by the field. For a wave propagating in a multilayer medium composed of two materials with different indices of refraction, multiple reflections, and interference effects will affect the phase accumulated upon transit. This is also true for a single material with end faces. For these cases, it is helpful to assign an ''effective index of refraction'' to the composite. The variation of the effective index of refraction with wavelength is the geometrical dispersion. A recent example of the useful application of geometrical dispersion is the ability to achieve phase matching for second harmonic generation in multilayer structures [7]. In PBG materials, the dispersion associated with the geometry of the composite dominates the material dispersion of the constituents. Another complicating factor with PBG materials is the finite size of the samples, in some cases only a few lattice periods in extent. For these finite-size structures, the dispersion relation can be quite different from that of an infinite structure.

In this paper, we specifically refer to the term *transit time* as the time required for the peak of the pulse to propagate through the length of the sample, or, more precisely, the time interval between the peak of the pulse entering the sample and the peak of the pulse exiting the sample. This assumes that the peak is well defined and measurable. In our experiment, we measure the time required for the pulse to propagate through free space from the laser source to the detector. Next, we place the sample in the optical path and record the new time. The difference in these two measurements is the *delay time*. For most materials, even those having anomalous dispersion, the delay time is positive because the refractive index of the material is greater than air and most values of anomalous dispersion are not large enough to offset the refractive index. The determination of the experimental transit time requires a measurement of the sample thickness which can be accurately measured to within a few micrometers with a vernier caliper. The actual transit time is then the measured delay time plus D/c, where D is the thickness of the sample.

In our previous work [8], we measured the transit time of a pulse propagating through a one-dimensional PBG sample of GaAs/AlGaAs. The group velocity was found to vary from $0.1c$ to $0.8c$ in the vicinity of the photonic band edge. In that work, the time calibration of the experimental apparatus was checked by measuring the transit time of a pulse propagating through a GaAs substrate. The longitudinal extent of each pulse was much less than the GaAs substrate thickness. In this situation, étalon effects are not important because the bandwidth of the pulse is much wider than the spacing of the transmittance resonances. The measured group velocity was found to be that of bulk GaAs.

The motivation of our previous work was to explore the potential of PBG materials as compact, tunable optical delay lines. Based on the positive outcome of the delay measurements we redesigned the measurement apparatus in a configuration more in keeping with the envisioned true time delay device. We replaced the high peak power actively mode locked erbium fiber laser with a simple injection current modulated external cavity diode laser. Thus, we went from picosecond, transform limited pulses to nanosecond, chirped pulses. In the present experiment, the length of the optical pulse is much larger than the length of the samples, approximately two orders of magnitude longer. Also, the laser wavelength is tunable by means of a grating in the external cavity. Initially, we discounted the effects of chirp on the transit time because the magnitude of the chirp, ~ 1 GHz, was more than two orders of magnitude smaller than the spacing of the transmittance maxima, ~ 100 GHz for the GaAs sample used in this work. Also, the chirp was only a small perturbation on the carrier frequency, the magnitude of the chirp being five orders of magnitude smaller than the carrier frequency.

On calibrating our new time measurement system with reference samples of bulk GaAs and silica, we found that étalon effects were important because the transit time of the peak of the pulse varied with the wavelength. Calculations based on transform limited pulses indicated that the range in the transit times should vary about the static transit time without the étalon effects. For the 450 μm thick GaAs sample, the theoretical transit time as a function of wavelength should range from 2.7 ps to 9.2 ps. We actually measured transit times ranging from -7 ps to $+22$ ps for the GaAs sample. As we will show, superluminal, zero, and negative transit times are to be expected if we consider all the parameters associated with the evolution of the pulse.

II. SAMPLES AND EXPERIMENTAL APPARATUS

The samples used in the transit time measurements consisted of a silica optical flat, 9.9 mm thick, and a polished GaAs substrate 0.45 mm thick. The surfaces were not antireflection coated and therefore had some residual reflection resulting in étalon effects. The theoretical transmittance spectra for the two samples are shown in Fig. 1. The optical constants for silica and GaAs were taken from Palik [9]. Transmittance maxima are separated by 0.085 nm (11 GHz) for the silica sample and 0.79 nm (99 GHz) for the GaAs sample.

The experimental arrangement for measuring the transit time of the optical pulses is shown in Fig. 2. The laser diode was tunable from 1505 to 1595 nm by means of an external grating (New Focus, Inc., Tunable Laser, Model 6328). The relatively small beam diameter did not permit tuning through the transmission resonances by tilting the sample. Using an optical spectrum analyzer with a 15 GHz free spectral range and a finesse of 150, we measured the laser wavelength stability to be better than 0.004 nm over several minutes.

Optical pulses were obtained by applying a Gaussian voltage pulse, 340 ps full width at half maximum (FWHM), from a pulser (Avtech Electro Systems, Model AVM-1-C-D-DSRCA). The repetition rate of the pulser was 10 MHz. Each voltage pulse was split into two paths, one to trigger the wave form digitizer and the other to modulate the laser diode current to produce a fast optical pulse. For the sample

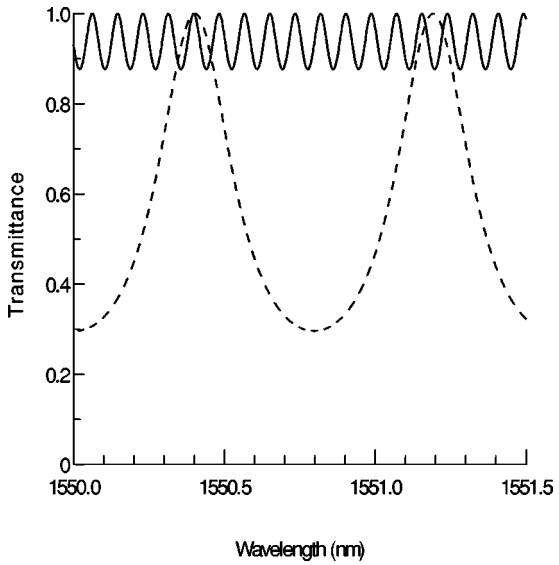

FIG. 1. Theoretical transmittance of the two samples. Solid line: transmittance of the silica optical flat, 9.9 mm thick; dashed line: transmittance of the GaAs wafer, 0.45 mm thick.

measurements, the laser was idling in cw mode at 50 mA (12 mA above threshold) and the voltage pulse was estimated to drive the laser from 50 mA to a peak current of about 70 mA.

The sample was positioned between the laser head and a high speed detector (New Focus, Model 1611 InGaAs detector with a 1 GHz bandwidth and a 400 ps rise time). The detector output was observed on a HP54750A digitizing oscilloscope having a HP54751A, 20 GHz module with a combined trigger and time base jitter of <2.5 ps. The total path without the sample served as the baseline. The sample was then inserted into the optical path and the time difference recorded.

The FWHM of the optical pulse was measured to be considerably longer than the voltage pulse injected into the laser. We checked the optical wave form using a 25 GHz detector (New Focus Model 1437) and found no distortion resulting from the 1 GHz detector. We attributed the pulse broadening to the bandwidth of the laser modulation circuit itself, which was only rated for a 300 MHz input. The optical pulse was roughly a Gaussian with a 1 ns FWHM.

For the transit time measurements we recorded the central portion of the wave form spanning a 500 ps time interval. The digitizing oscilloscope was set to average 16 wave forms for each wavelength measurement. The acquisition time per

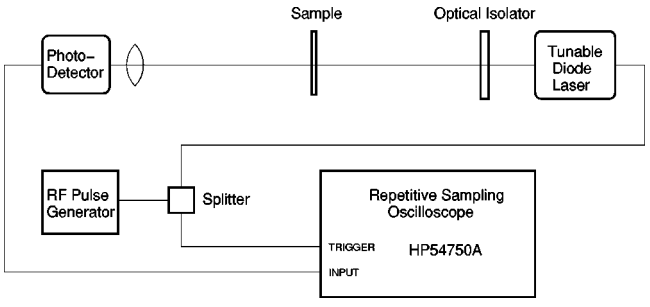

FIG. 2. Experimental apparatus for measuring the transit times.

wavelength was ~ 10 s. The stored wave form consisted of 513 data points to provide a 1 ps time resolution. The wave form was fitted to a third order polynomial to determine the peak position of the pulse in time.

III. EXPERIMENTAL TIMING CORRECTIONS

The measurements required that the timing resolution of the system be on the order of 1 ps. Effects that were found to influence the transit time versus wavelength measurement include thermal drift of the oscilloscope time base, optical feedback into the laser cavity, position of the focal spot on the detector, detector rise time as a function of pulse intensity, interference effects of optical elements, and cavity dwell time effects of the laser.

The ambient temperature of the laboratory was found to affect the delay measurement at a rate of 3.5 ps per 1 °C temperature change. The long electrical transmission lines had a weak thermal dependence of 0.7 ps per 1 °C. The main source of the thermal drift was traced to the oscilloscope. It was remedied by maintaining a constant temperature in the laboratory and recording data after a 2 h warm up time.

Weak optical feedback into the laser caused power fluctuations on the order of 10% resulting in timing jitter. An optical isolator with 46 dB of isolation reduced the power fluctuations below 1% and eliminated this problem.

The high speed detector had a lens mounted on the front end to focus the beam. It was noticed that small position changes of the laser beam on the detector resulted in large timing variations. We also found that the laser beam position oscillated slightly as the laser was tuned in wavelength. Subsequently, we mounted the detector on a translation stage and determined the timing dependence on detector position to be 0.5 ps per 1 μm of translation. A fiber pigtailed detector eliminated the timing dependence of the spatial beam position.

The detector rise time and therefore the peak position of the pulse were found to be dependent on the strength of the optical signal impinging on the detector. The time measurement varied by 4 ps if the detector signal doubled. This dependence on signal strength was greatly reduced if the optical signal on the detector was modest. For the smaller signal levels used in the experiment the power dependence could be neglected.

A final source of timing error resulted from the laser itself. Baseline measurements of transit time without a sample in the optical path displayed strong wavelength dependence. The measured transit time had oscillations on the order of 25 ps with a period of 0.4 nm (or 50 GHz at a wavelength of 1550 nm). Therefore, the laser itself was a tunable delay line with a range of 25 ps. Also, the laser delay was dependent on the injected current, with larger timing variations for the higher drive currents. The 0.4 nm periodicity was identical to the periodicity observed in the laser power versus wavelength spectrum which had power oscillations of $\approx 10\%$. According to the manufacturer, the laser diode had one facet coated with a high reflector and the other facet was antireflection (AR) coated. The AR coating is not perfect and results in a small residual reflection. This weak étalon effect

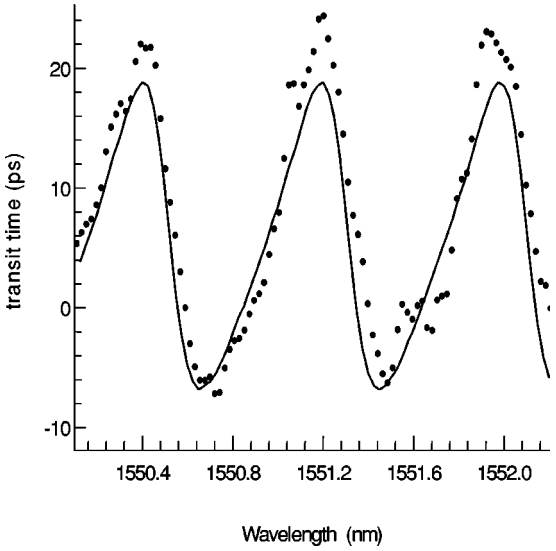

FIG. 3. Experimental transit times for the GaAs sample (data points). Also shown is the theoretical transit time spectrum (solid line).

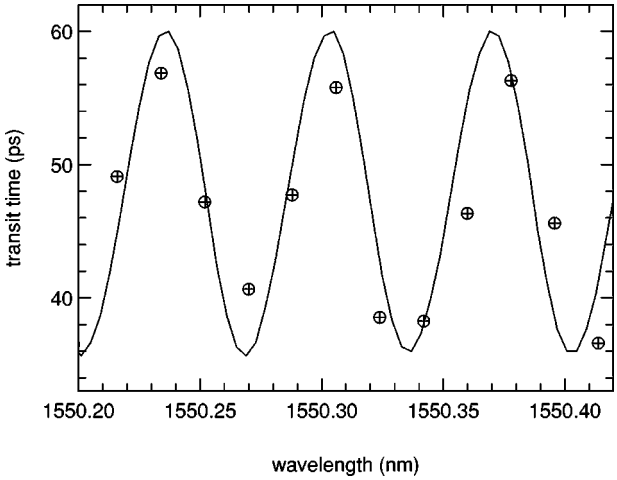

FIG. 4. Experimental transit times for the silica sample (data points). Also shown is the theoretical transit time spectrum (solid lines).

changes the cavity Q or dwell time and causes the laser power to oscillate on the order of 10% as the wavelength is scanned. These power oscillations will shift in wavelength depending on the exact temperature of the diode and other factors. To properly account for this, we recorded a baseline scan before every set of measurements.

We also corrected the transit time spectra for an error in the wavelength step precision of the laser. Software for scanning the laser's wavelength over a specified range and acquiring the detector signal was developed to provide automated spectral measurement capability. The laser wavelength was stepped in 0.02 nm (2.5 GHz) intervals and then a wave form was recorded. This was the smallest interval for the tunable laser. Using an optical spectrum analyzer, we tracked the actual step interval to be on average 0.018 nm with a standard deviation of 0.004 nm. The optical spectrum analyzer was removed when recording the transit time spectra to reduce extraneous reflections, but we corrected the transit time data for the overall wavelength scan error of 10%. The slight variation in sequential step size coupled with the inherent time variation of the laser pulse with wavelength was the major source of error in the transit time measurements. Based on the above analysis, we estimated the time delay accuracy as a function of wavelength to be 1 to 2 ps.

IV. EXPERIMENTAL TRANSIT TIMES

Figures 3 and 4 show the experimental results of the transit times for the chirped pulses propagating through the GaAs and silica samples, respectively. The experimental data points are limited by the minimum wavelength step of the laser, 0.018 nm, which means that the silica data are undersampled. In spite of the limited number of data points for the silica sample, the measurements show the dynamic behavior of a pulse propagating through a linear medium with boundaries. If the samples had antireflection coatings or if the optical pulse length was less than the thickness of the sample, the transit times shown in Figs. 3 and 4 would be independent of wavelength. For reference, the transit time of a pulse propagating a distance of 450 μm in bulk GaAs is 5.1 ps neglecting material dispersion and 5.6 ps including the effects of material dispersion. We measured transit times ranging from -7 ps to $+22$ ps for the GaAs sample. The variation in transit times as a function of wavelength results from the geometrical dispersion associated with reflections at the boundaries. Transit times of less than 5.6 ps are superluminal. For 0 ps transit times, the peak of the transmitted pulse exits the sample at the same instant the incident pulse arrives at the sample. Negative transit times indicate that the peak of the transmitted pulse has already exited the sample before the peak of the incident pulse arrives at the sample. Another unusual feature is that the minimum transit time, -7 ps, does not occur at the minimum in the transmittance, which is 30%, but occurs at a transmittance of 55%.

For the silica sample, the transit times range from 36 ps to 60 ps. The time required for a pulse to propagate 9.9 mm through a material of index of refraction 1.444 (silica) is 47.7 ps if we neglect material dispersion. Adding the material dispersion of silica results in an additional 0.6 ps for a transit time of 48.3 ps (superluminal threshold).

Both the GaAs and silica samples display superluminal behavior at relatively high values of transmittance. In the following section we will describe a theoretical model to calculate the transit times for transform limited pulses and chirped pulses and elucidate the actual impact of the chirp on the transit times.

V. MODELING THE CHIRP PROFILE OF THE INCIDENT PULSE

As we did not have a direct measure of the chirp, the semiconductor rate equations were solved to determine the chirp profile of the laser pulse. These equations have been extremely successful in describing the characteristics of diode lasers. The rate equations for the complex field E and carrier density n for the laser can be written as

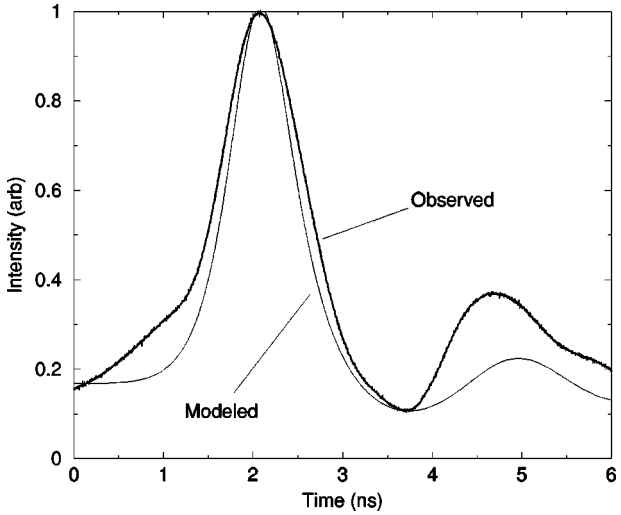

FIG. 5. Comparison of the measured optical pulse profile and theoretical pulse profile calculated from the laser rate equations.

$$\frac{dE}{dt} = \frac{1}{2}(1+i\alpha)G_N(n-n_{\rm th})E, \tag{1}$$

$$\frac{dn}{dt} = \frac{I}{eV_a} - \frac{n}{\tau_s} - \left(\frac{1}{\tau_p} + G_N(n-n_{\rm th})\right)|E|^2, \tag{2}$$

and the parameters α, G_N, $n_{\rm th}$, I, e, V_a, τ_s, and τ_p represent the linewidth enhancement factor, differential gain, threshold carrier density, pump current, electron charge, active volume, carrier lifetime, and photon lifetime of the laser, respectively [10]. We used parameters for a typical semiconductor laser: $\alpha=5.0$, $G_N=2.6\times10^{-6}$ cm^3/s, $n_{\rm th}=1.5\times10^{18}$ cm^{-3}, $\tau_s=700$ ps, and $\tau_p=3$ ps. The active volume V_a is determined from the laser threshold current $I_{\rm th}$ and the parameters given above. The rate equations were solved using a Gaussian pump current profile $I(t)$, with the same width measured for our optical pulse, 1 ns, and a peak current of 20 mA, superimposed on a baseline current of 55.3 mA. The measured threshold current for our laser at the typical operating wavelength was $I_{\rm th}=46.1$ mA. The change in frequency of the laser, i.e., the chirp, is given by $\Delta\omega = d\phi(t)/dt$.

The chirp profile, and therefore the transit time spectrum, will be most sensitive to the linewidth enhancement factor since it determines the strength of the coupling between the phase and the amplitude of the field. Typical values for the linewidth enhancement factor range from 4 to 6. We chose a value of 5 for the calculation. For other values of the linewidth enhancement factor, the fit to the experimental transit times is slightly worse.

Figure 5 shows the comparison of the measured optical pulse profile and the theoretical pulse profile obtained from the laser rate equations. The pulse ringing observed in Fig. 5 is due to relaxation oscillations associated with the fluctuations in the electron density.

The relaxation oscillations in the optical pulse profile result in a ringing of the chirp profile. To simplify the calculations of the transit time, the optical pulse shown in Fig. 5 was truncated and fitted to a Gaussian and the corresponding chirp calculated. The chirp profiles for the full pulse and the truncated pulse are shown in Fig. 6. The most important feature of the chirp profile in relation to the transit time is the central slope of the chirp.

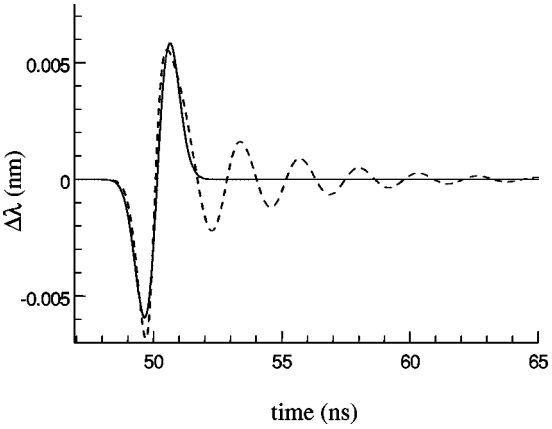

FIG. 6. Chirp profile derived from the laser rate equations for a 1 ns long (FWHM) optical pulse, dashed line. Input parameters for the rate equations are based on the operating parameters of the laser used in the transit time measurements. The *x*-axis offset is arbitrary. The solid curve is the simplified chirp profile used in the calculation of the transit time.

A graphic illustration of the relative size of the chirp is shown in Fig. 7. In the figure are plotted the theoretical transmittance for the GaAs and silica samples along with the power spectra of two pulses. The narrow power spectrum is for a 1 ns long (FWHM) transform limited pulse while the broader power spectrum has the same pulse duration, 1 ns, but includes the chirp profile of Fig. 6.

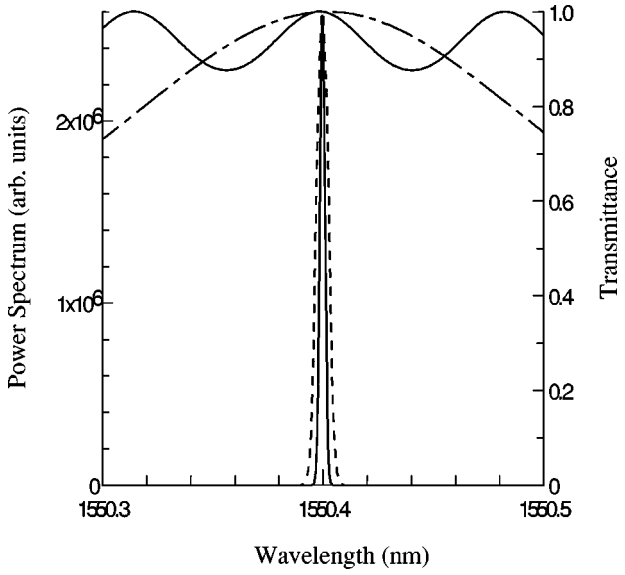

FIG. 7. Theoretical power spectrum of a transform limited, 1 ns long (FWHM) Gaussian pulse (solid line) and the same pulse with chirp (dashed line). The chirp profile is shown in Fig. 6. Superimposed above the power spectrum are the transmittance of the GaAs sample and the silica sample.

VI. TRANSIT TIME CALCULATIONS

We now outline the procedure that we use to calculate the transmissive properties of the structure under consideration. The method is based on the matrix transfer method. The transmission is generally defined as the ratio of the transmitted to incident fields [11], that is,

$$\tilde{t}(\omega)=E_{\mathrm{out}}(\omega)/E_{\mathrm{in}}(\omega). \tag{3}$$

We can recast Eq. (3) as follows:

$$E_{\mathrm{out}}(\omega)=\tilde{t}(\omega)E_{\mathrm{in}}(\omega). \tag{4}$$

The function $\tilde{t}(\omega)$ can be viewed as a propagator that is calculated using the matrix transfer method. Taking the Fourier transform, it follows that

$$E_{\mathrm{out}}(t)=\int_{-\infty}^{+\infty}\tilde{t}(\omega)E_{\mathrm{in}}(\omega)e^{-i\omega t}d\omega, \tag{5}$$

where $E_{\mathrm{out}}(t)$ is the temporal profile of the transmitted field, and $E_{\mathrm{in}}(\omega)$ is the Fourier transform of an *arbitrary* incident field. Therefore, once the transmission function has been calculated by the matrix transfer method, all relevant information about the transmitted field can be extracted.

In the current experiment, the incident field is of the form

$$E_{\mathrm{in}}(t)=E_0\exp\left[-\frac{t^2}{2\tau_0^2}-i\omega t-i\phi(t)\right], \tag{6}$$

where $\phi(t)$ is a Gaussian chirp introduced by modulating the injection current of the laser diode and τ_0 is related to the τ_{FWHM} of the pulse intensity by $\tau_0=\tau_{FWHM}/(2\sqrt{\ln 2})$. To determine the transit time, we calculate the output field for free space propagation of distance D and then calculate the output field for propagation through the sample of thickness D. The time difference between the two peaks of the output field is the delay time. Adding D/c to the delay time gives the actual transit time for the pulse. We calculated the transit time for transform limited pulses as well as chirped pulses to elucidate the effect of the chirp.

While the above procedure provides the required data on the transit times, it is not very helpful in understanding the physical processes leading to the delay. For better insight it is helpful to calculate the *effective* index of refraction for the samples. When light propagates through the GaAs or silica sample, some of the energy is lost due to reflection and, in addition, the transmitted field accumulates a phase upon transit. We treat the sample as a black box and ask, ''What is the effective index of refraction that will provide the proper phase and amplitude of the transmitted field?'' The effective index is complex and has a real component to account for the phase and an imaginary component to account for the loss. For example, we treat the silica sample, which has only a real index of refraction and length D, as an effective material with a complex index of refraction and length D. Hence, the sample is transformed into an absorptive material that has no reflections at the boundaries. The effective index provides us with the geometrical dispersion relation for the sample and hence insight into the group velocity and the transit time. The effective index point of view is also helpful for other applications such as phase matching in photonic band gap crystals for second harmonic generation [7].

In order to calculate the effective index, we use the procedure outlined in Ref. [7]. With the effective index we can use the standard expression for group velocity to determine the transit time spectra. The group velocity V_g is related to the phase velocity V_p and dispersion $dn/d\lambda$ by

$$V_g=V_p\left[1+\frac{\lambda}{n}\frac{dn}{d\lambda}\right], \tag{7}$$

where λ is the wavelength in the medium. In terms of the free space wavelength λ_0,

$$V_g=V_p\left[1-\frac{\lambda_0}{n}\frac{dn}{d\lambda_0}\right]^{-1}. \tag{8}$$

Thus, the highly dispersive regions in the effective index spectra correspond to the extremes in the transit times.

As we will see, an evaluation using the effective index approach is adequate to predict transit times for transform limited pulses but not for chirped pulses. The correct evaluation of the transit time for chirped pulses is done by integrating Eq. (5), where the input field is taken to be a chirped Gaussian pulse. The picture that emerges is that chirping the input field causes additional effects that modify the transit time, leading to a fourfold increase in the range of transit times as well as negative transit times. Also, surprisingly, there is no distortion in the shape of the transmitted pulse.

We note that the matrix transfer method is a steady-state approach. Although it is for plane waves, one can always do a Fourier decomposition of a pulse. Since we are in a linear regime the method has no approximations. We also checked the matrix transfer method against a beam propagation model (BPM) and obtained identical transit times.

The effective index model is an approximation when applied to pulses and requires the spectral content of the pulse to be smaller than the features in the transmittance. This is a reasonable approximation for our experimental conditions.

VII. THEORETICAL RESULTS

The theoretical results for the GaAs and silica samples are shown in Figs. 8 and 9, respectively. Four curves are plotted; the transmittance, the effective index of refraction, the transit time for a transform limited pulse, and the transit time for a chirped pulse.

A. Effective index of refraction

We want to point out that the effective indices for the two samples amount to a very small oscillation about the bulk index of refraction of the material. For the GaAs the effective index varies by 3×10^{-4} and for silica the effective index varies by 2×10^{-6}. At first glance this seems to be an insignificant perturbation on the bulk index, but when combined with the fact that the effective index oscillates with such a small period, the effect on the dispersion is huge. As

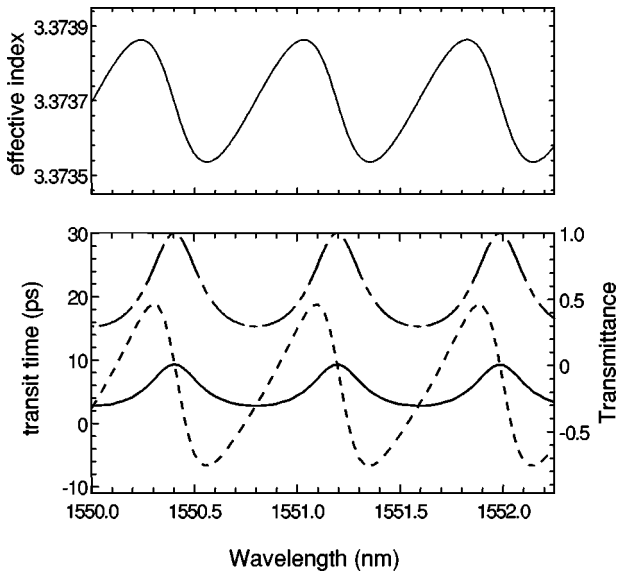

FIG. 8. Theoretical results for the GaAs sample. Plotted are the transmittance (long-short dashes), effective index (upper figure), transit time for the transform limited pulse (solid line), and transit time for the chirped pulse (dashed line).

shown in Table I, the geometrical dispersion due the reflections at the air/medium interfaces can easily be a factor of 5 larger than the bulk material dispersion and can be of opposite sign. Because the material dispersion is much smaller than the geometrical dispersion, the material dispersion was not considered in any of the calculations of this paper in order to clarify the effect of the geometrical dispersion. We included the material dispersion in the transit time calculations to test the validity of this approximation and found that the material dispersion had a negligible effect on the overall results.

Note that, at the minima and maxima in the transmittance spectra of Figs. 8 and 9, the magnitude of the dispersion is largest. In these regions we expect the largest deviations in transit time compared with a bulk medium having antireflection coatings. Also note that the points of inflection in the transmittance spectra are the points corresponding to the maximum and minimum values of the effective index of the samples. If the points of inflection are not spaced at equal wavelength intervals, the result is an asymmetry in the effective index spectra. This asymmetry can be seen in the GaAs effective index spectrum of Fig. 8, which has a sawtooth profile. The silica sample has an effective index spectrum more sinusoidal in nature.

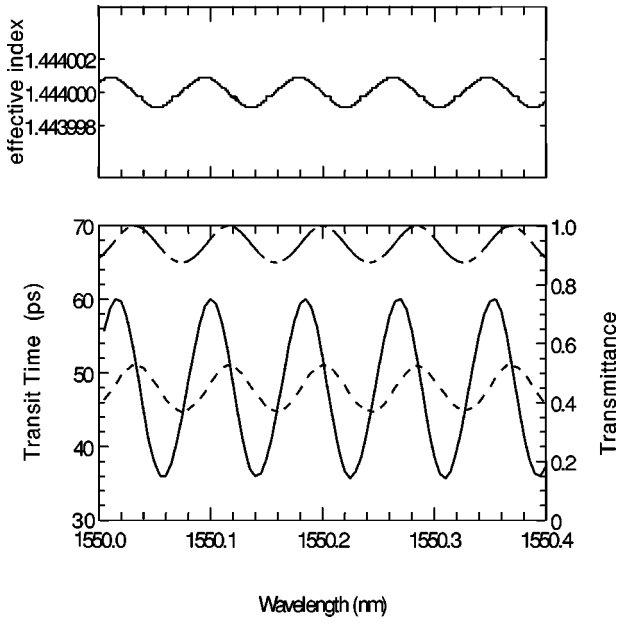

FIG. 9. Theoretical results for the silica sample. Plotted are the transmittance (long-short dashes), effective index (upper figure), transit time for the transform limited pulse (solid line), and transit time for the chirped pulse (dashed line).

B. Transit times of transform limited pulses

The solid curve in Figs. 8 and 9 show the theoretical transit times for a transform limited pulse propagating through the samples. The transit times calculated from Eq. (5) (matrix transfer method) and Eq. (8) (standard expression for group velocity using the geometrical dispersion) yield the same results.

We first note that transmittance maxima correspond to the longest transit times and transmittance minima correspond to the shortest transit times. For unity transmittance, we have a resonant cavity and an associated long dwell time.

We can now see the strong influence of geometrical dispersion on the transit time of the transform limited pulses. In both the GaAs and silica samples, the material dispersion causes ≈ 0.5 ps increase in the transit time, while the geometrical dispersion causes the transit time to vary by about 6 ps into subluminal and superluminal regimes.

C. Transit times of chirped pulses

The chirped pulse transit times were calculated from Eq. (3) using the chirp profile generated by the laser rate equations. The theoretical transit times for chirped pulses, the dashed curve in Figs. 8 and 9, are very different from transform limited pulses. The obvious differences are the much larger transit time ranges for chirped pulses and a wavelength shift in the maximum and minimum transit times. In both the GaAs and the silica samples, the range in transit times increases fourfold, from 6 ps to 24 ps, for the chirped pulses compared with transform limited pulses. The modifications in the transit times are due to the wavelength dependence of the transmittance and the chirp profile of the pulse.

In calculating the transit time for various chirp profiles we find that the most significant feature is the strength of the chirp at the center of the pulse, Fig. 6. In fact, approximating the chirp profile near the center of the pulse with a linear chirp across the entire pulse yields the same theoretical transit times. As the magnitude of the chirp tends toward zero, the transit times approach that of the transform limited pulse. At the transmittance maxima and minima, the initial chirp of the incident pulse has no effect on the transit time.

In previous work by D'Aguanno *et al.* [12], it was shown that the transit time for chirped pulses depends on the prod-

TABLE I. Summary of the sample parameters and transit times.

	GaAs	Silica
Sample length	0.45 mm	9.9 mm
Refractive index (at $\lambda_0 = 1.55 \mu$m)	3.3737	1.444
Transmittance resonance width (FWHM)	0.25 nm (31 GHz)	0.041 nm (5.1 GHz)
Transmittance minimum	30%	88%
Bulk material dispersion ($\Delta n/\Delta\lambda_0$)	$-0.19\ \mu\text{m}^{-1}$	$-0.012\ \mu\text{m}^{-1}$
Transit time for bulk material	5.6 ps	48.3 ps
Geometrical dispersion ($\Delta n/\Delta\lambda_0$)	-1.8 to $+1.0\ \mu\text{m}^{-1}$	-0.06 to $+0.06\ \mu\text{m}^{-1}$
Transit time for transform limited pulse	2.7 to 9.2 ps	45 to 51 ps
Transit time for chirped pulse	-6.5 to $+18.5$ ps	36 to 60 ps

uct of the slope of the transmittance spectrum, the strength of the chirp, and the square of the pulse duration. Surprisingly, the pulse remains Gaussian, at least to a first order approximation.

We point out that the changes in the chirp profile of the pulse due to the transit through the medium are quite small. A plot of the chirp profile for the incident and transmitted pulse shows the two to be identical, that is, much smaller than a 1% change.

While the differences in chirped pulse transit times of the GaAs and silica samples appear profound, such as negative transit times, there are similarities. For example, the range of transit times is nearly identical for the two samples. The explanation for this similarity can be traced to the slope of the transmittance spectrum. As seen in Fig. 1, the maximum rate of change in the transmittance is about the same in both samples. Looking at the phenomenon from this point of view, the main difference in the behavior of the two samples is due to the length of the sample and the bulk refractive index, which set the average transit time. A slightly deeper transmittance minimum in the GaAs sample would provide negative transit times even for transform limited pulses.

VIII. COMPARISON OF THEORY AND EXPERIMENT: TRANSIT TIMES AND PULSE DISTORTION

Figures 3 and 4 show the experimental and theoretical results of the transit times for the chirped pulses propagating through the GaAs and silica, respectively. The theoretical data are based on a 1 ns long pulse with the chirp profile shown in Fig. 6. The predicted fourfold increase in the transit time range for chirped pulses agrees quite well with the experimental results. The experimental superluminal and negative transit times also agree with the theoretical predictions.

In the GaAs spectrum, a sawtooth transit time spectrum is observed as predicted by the theory. The primary discrepancy with theoretical predictions in the GaAs spectrum is that the longest measured transit times are about 4 ps longer than predicted by theory.

Up to this point we have focused on the transit time of the peak of the pulse and demonstrated that a chirped pulse has an increased transit time range compared with transform limited pulses. For a transform limited Gaussian pulse, the frequency components are spread uniformly throughout the pulse and the pulse remains Gaussian after propagating through the medium, assuming that the spectral content of the pulse is much smaller than the width of the absorption line [2]. The only change in the pulse envelope is the amplitude. Surprisingly, the same conditions hold for chirped pulse propagation. The transmitted pulse envelopes calculated from Eq. (5) show no distortion when compared to the Gaussian input pulse. The only change in the pulse is the amplitude. We also calculated wave forms using the entire pulse including the relaxation oscillations to see if other than Gaussian pulses might show some distortion. The result was the same: no pulse distortion was evident for the transmitted pulse.

A comparison of the experimental output pulse and input pulse is shown in Fig. 10. If distortion is present, we expect it to occur where the transit time deviates most from the transform limited pulses. The particular case plotted in Fig. 10 is at a wavelength in the vicinity of the longest transit time. The only noticeable distortion is in the wings of the pulse. We attribute this to the fact that the laser is strongly overdriven. The laser head is packaged for a maximum input modulation frequency of 300 MHz, and we are applying a 340 ps voltage pulse in order to obtain the shortest laser

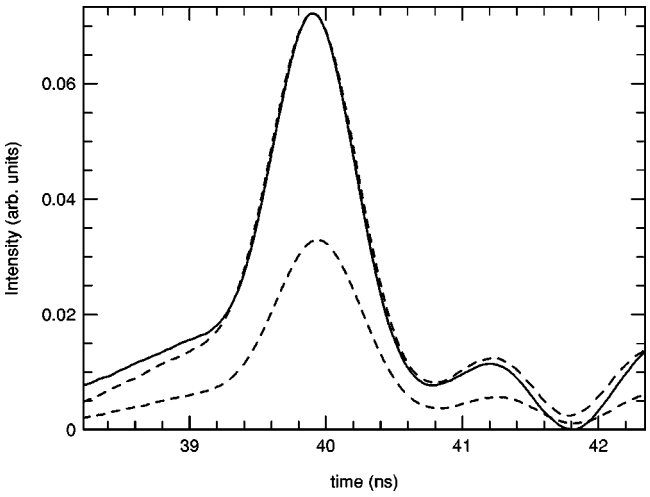

FIG. 10. Comparison of experimental input and output pulses at a wavelength in the region of longest transit time. The measured output pulse (dashed line) was scaled in amplitude and translated in time in order to better compare it with the input pulse (solid line). The output pulse is also shown before the scaling procedure.

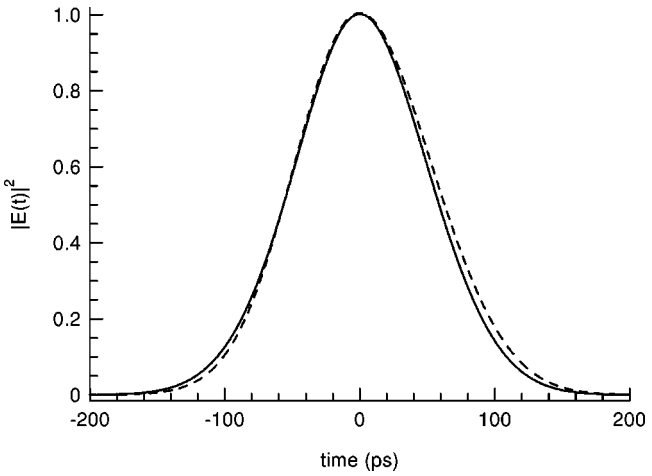

FIG. 11. Comparison of a 100 ps duration input pulse and output pulse at a wavelength in the region of longest transit time. The output pulse (dashed line) was scaled in amplitude and translated in time in order to better compare it with the input pulse (solid line).

pulse duration. As shown in Fig. 5, which compares the pulse profile predicted from the laser rate equations and the experimental pulse profile, the discrepancies are most obvious in the wings of the pulse and in the relaxation oscillations. We expect that pulses from lasers packaged for high speed operation would not display distortion in the pulse wings.

For applications as time delay devices, we should consider the range of transit times with respect to the duration of the pulse or, in other words, how much can we vary the pulse in time in terms of its FWHM. In our measurements, the ratio of the transit time range to the pulse duration is (25 ps/1000 ps) 2.5%. The next question would be, ''How much can we increase this ratio without significant pulse distortion?'' As an illustration we calculated the transit times and pulse shapes for a 100 ps long pulse transmitted through the GaAs sample. The chirp was adjusted to maintain the 25 ps transit time range. Since the pulse was shortened by a factor of 10, the chirp was increased by 100. The resulting power spectrum for the 100 ps pulse had a FWHM of 12 GHz. This is quite a broad spectrum since the transmittance resonance of the GaAs samples has a 31 GHz FWHM. Figure 11 shows the comparison of the 100 ps long input pulse and output pulse in the vicinity of the longest transit time. Here we can just begin to see the effects of pulse shaping by the interaction of the chirp profile and the transmittance spectrum. The high frequency components of the leading edge of the pulse are slightly attenuated, while the low frequency components on the trailing edge have a higher transmittance. A pulse tuned to the minimum transit time shows similar distortion but in reverse. Considering that the frequency content of the pulse is 40% of the width of the transmittance resonance, the distortion is unexpectedly small. With this simple system of a chirped pulse and an étalon, it is possible to achieve a tuning range of 25% of the width of the input pulse.

As noted in a recent article by Kuzmich *et al.* [13] the meaning of *front velocity* and *signal velocity* can be defined for pulses having a leading edge in the form of a step function. Unfortunately, for Gaussian pulses these terms are not well defined. What we can say is that, for the same input pulse, the leading edge of a pulse that was transmitted through the sample always lags behind the leading edge of a pulse that propagated an equal physical distance through the vacuum. Therefore, neither the signal velocity nor the front velocity exceeds the speed of light in vacuum and the measured transit times apply to the group velocity.

IX. SUMMARY AND CONCLUSIONS

We have demonstrated that the transit times of electromagnetic pulses propagating through a medium of finite length are strongly influenced by geometrical dispersion. Even in the simple case of a pulse propagating through a silica flat having reflectivities of only 3.3% per interface, the transit time variations as a function of wavelength are large. For a transform limited pulse the effects of geometrical dispersion cause the transit time to be anywhere from 45 to 51 ps depending on the specific wavelength. If the electromagnetic pulse is generated by modulating the injection current of a laser diode, then the transit time range is 36 to 60 ps due to the chirp on the incident pulse. Thus, the geometrical dispersion and associated transmittance spectrum cause a 50% variation in the transit time of the chirped pulses compared with the static transit time for material dispersion alone. These are significant variations considering that the transmittance spectrum varies only 12%, from a minimum of 88% to a maximum of 100%.

The transit time variations appear more dramatic in the case of GaAs, which has a geometrical dispersion more than an order of magnitude larger than silica (Table I). The geometrical dispersion results in a transit time range of 2.7 to 9.2 ps for transform limited pulses and -7 to $+22$ ps for chirped pulses. In the case of the chirped pulse, this is a 450% variation in the transit time relative to the static transit time with material dispersion. For the transform limited pulse, it is a 100% variation about the transit time value resulting from material dispersion alone. In GaAs, the geometrical dispersion and associated transmittance spectrum can provide negative transit times depending on the specific wavelength while providing relatively high values of transmittance.

A final point with regard to the tuning range: to achieve the full tuning range for the transform limited pulse, the corresponding transmittance would be 100% for the longest transit time and the minimum value of transmittance for the shortest transit time. For the chirped pulse, the full tuning range can be achieved with much higher values of transmittance due to the shift in the transit time spectra compared with the transform limited pulse. The entire tuning range of the GaAs sample can be achieved with a minimum transmittance of 55% instead of the 30% for a transform limited pulse. Thus, with the simple system of a laser diode source and a GaAs substrate we can show superluminal and negative transit times at greater than 50% transmittance without

any distortion in the shape of the transmitted pulse.

The large increase in the transit time range for chirped pulses may prove useful for applications in optical phased arrays, optical control of microwaves, and control of polarization modal dispersion in high bit rate optical fiber networks.

Active control of the transit time can be achieved by changing the wavelength of the laser source, the thermo-optic effect, or in the case of GaAs by the electro-optic effect. A GaAs waveguide 450 μm long would require an index change of only 3×10^{-4} to span the full transit time range.

[1] L. Brillouin, *Wave Propagation and Group Velocity* (Academic Press, New York, 1960).
[2] C. G. B. Garrett and D. E. McCumber, Phys. Rev. A **1**, 305 (1970).
[3] D. Stroker, J. Huve, and F. Mitschke, Appl. Phys. B: Lasers Opt. **69**, 323 (1999).
[4] A. M. Steinberg, P. G. Kwiat, and R. Y. Chiao, Phys. Rev. Lett. **71**, 708 (1993).
[5] G. D'Aguanno, M. Centini, M. Scalora, C. Sibilia, M. J. Bloemer, C. M. Bowden, J. W. Haus, and M. Bertolotti, Phys. Rev. E **63**, 036610 (2001).
[6] J. Opt. Soc. Am. B **10**, 279 (1993), special issue on photonic band gaps.
[7] M. Centini, C. Sibilia, M. Scalora, G. D'Aguanno, M. Bertolotti, M. J. Bloemer, C. M. Bowden, and I. Nefedov, Phys. Rev. E **60**, 4891 (1999).
[8] M. Scalora, R. J. Flynn, S. B. Reinhardt, R. L. Fork, M. J. Bloemer, M. D. Tocci, C. M. Bowden, J. P. Dowling, and R. P. Leavitt, Phys. Rev. E **54**, R1078 (1996).
[9] E. D. Palik, *Handbook of Optical Constants of Solids* (Academic Press, Orlando, FL, 1985).
[10] G. P. Agrawal and N. K. Dutta, *Semiconductor Lasers* (Van Nostrand Reinhold, New York, 1993).
[11] G. R. Fowles, *Introduction to Modern Optics* (Dover, Mineola, NY, 1989).
[12] G. D'Aguanno, M. Centini, M. J. Bloemer, K. Myneni, M. Scalora, C. M. Bowden, C. Sibilia, and M. Bertolotti, Opt. Lett. **27**, 176 (2002).
[13] A. Kuzmich, A. Dogariu, L. J. Wang, P. W. Milonni, and R. Y. Chiao, Phys. Rev. Lett. **86**, 3925 (2001).